



Cite this: *Chem. Commun.*, 2018, 54, 2788

Received 17th January 2018,  
Accepted 14th February 2018

DOI: 10.1039/c8cc00393a

rsc.li/chemcomm

# The effect of geometric isomerism on the anticancer activity of the monofunctional platinum complex *trans*-[Pt(NH<sub>3</sub>)<sub>2</sub>(phenanthridine)Cl]NO<sub>3</sub>†

Wen Zhou,<sup>ab</sup> Mohammad Almeqdadi,<sup>b</sup> Michael E. Xifaras,<sup>b</sup> Imogen A. Riddell,<sup>‡a</sup> Ömer H. Yilmaz\*<sup>b</sup> and Stephen J. Lippard<sup>ib</sup>\*<sup>a</sup>

**A *trans*-DDP based monofunctional phenanthridine Pt(II) complex was synthesized and characterized. Its anticancer activity was studied *in vitro* on a panel of human cancer cell lines and mouse intestinal cancer organoids. This complex displays significant anti-tumor properties, with a different spectrum of activity than that of classic bifunctional cross-linking agents like cisplatin.**

Initially the development of platinum-based anticancer agents was focused on the synthesis and evaluation of complexes that obeyed structure–activity relationships (SARs)<sup>1</sup> set forth in the 1970's. From these studies, carboplatin and oxaliplatin were identified and both have gone on to receive worldwide approval as chemotherapeutics. Today they continue to play an important role in cancer treatment and management. However, the prevalence of inherent and acquired resistance to platinum treatment<sup>2–4</sup> requires the development of new complexes that operate through different mechanisms. Monofunctional DNA binding platinum(II) complexes represent an alternative class of very potent anticancer agents.<sup>5</sup> Unlike cisplatin and its derivatives, these complexes contain only one labile ligand and thus form a single covalent bond to DNA.

Pyriplatin, *cis*-diammine(pyridine)chloroplatinum(II), a monofunctional, cationic platinum(II) compound, displayed a spectrum of activity that differed from that of any of the clinically approved platinum drugs.<sup>6</sup> However, the overall potency of pyriplatin was much less than that of cisplatin in all cancer cell lines tested. We subsequently pursued a rational, structure-based approach for improving the potency of monofunctional platinum anticancer drugs.<sup>7</sup> By determining the X-ray structure of RNA polymerase II

stalled at a pyriplatin adduct on a short DNA duplex containing a bound RNA, they deduced that the pyriplatin–DNA adduct may prevent translocation from the active site and block RNA chain elongation because of steric interactions and hydrogen bonding with the bridge helix, operating by a mechanism of transcription inhibition that differs from that of *cis*-DDP. Based on this rationale, phenanthriplatin was designed, synthesized, and discovered to have significantly greater efficacy for killing cancer cells than either *cis*-DDP or oxaliplatin.<sup>6</sup> Moreover, according to the National Cancer Institute (NCI) cytotoxicity screening assay, phenanthriplatin exhibited a unique cancer cell-killing profile compared to all other platinum agents held in the NCI archives. The success of phenanthriplatin strongly encouraged further study of monofunctional Pt(II) compounds as anticancer drug candidates. In the present work, we report the synthesis and anticancer activity of a *trans*-DDP based monofunctional phenanthridine Pt(II) complex, in further pursuit of novel platinum cancer drug candidates.

*trans*-[Pt(NH<sub>3</sub>)<sub>2</sub>(phenanthridine)Cl]NO<sub>3</sub>, **1**, was prepared following the procedure developed for phenanthriplatin<sup>6</sup> and characterized by a variety of analytical methods, including <sup>1</sup>H and <sup>13</sup>C NMR spectroscopy, ESI-MS, and elemental analysis. Complex **1** was also structurally investigated by single crystal X-ray diffraction.

The solid-state study reveals that complex **1** adopts the expected square-planar coordination geometry with a *trans* arrangement of ammine ligands. Similar to phenanthriplatin, the plane of the phenanthridine ligand in complex **1** is approximately perpendicular to that of the platinum coordination plane (Fig. 1). The distance between the platinum atom and the overhanging carbon atom on the phenanthridine ligand (black arrow in Fig. 1) of complex **1** (3.224 Å) is nearly identical to that previously reported for phenanthriplatin (3.220 Å). This observation suggests that, like phenanthriplatin, complex **1** may show selectivity for nucleophilic binding sites on DNA while inhibiting unfavourable reactions with cytoplasmic sulphur nucleophiles.

We anticipated that, as with phenanthriplatin, the steric bulk of the phenanthridine ligand in complex **1** would impede procession of both DNA<sup>8</sup> and RNA<sup>9</sup> polymerases and may

<sup>a</sup> Department of Chemistry, Massachusetts Institute of Technology, Cambridge, MA 02139, USA. E-mail: lippard@mit.edu

<sup>b</sup> The Koch Institute for Integrative Cancer Research, Massachusetts Institute of Technology, Cambridge, MA 02139, USA. E-mail: ohyilmaz@mit.edu

† Electronic supplementary information (ESI) available. CCDC 1582154. For ESI and crystallographic data in CIF or other electronic format see DOI: 10.1039/c8cc00393a

‡ Current address: School of Chemistry, University of Manchester, Oxford Road, Manchester, M13 9PL, UK.



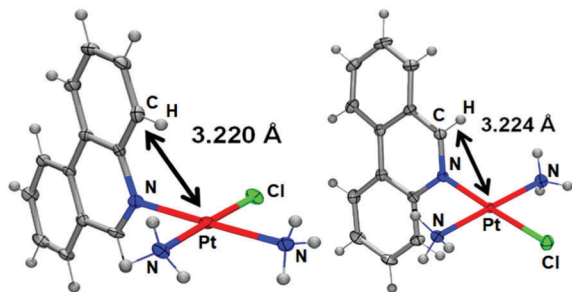


Fig. 1 Comparison of the X-ray crystal structures of phenanthriplatin (left) and **1** (right). The platinum–carbon distances shown reveal that these two complexes exhibit similar degrees of steric protection from incoming nucleophiles at the axial positions.

interfere with other essential enzymatic functions,<sup>10</sup> leading to potent anticancer activity. The *in vitro* anticancer activity of complex **1** was initially probed using fluorescence microscopy and the LIVE/DEAD cell assay, which is a combination of the ethidium homodimer-1 assay and staining with calcein AM (Fig. 2). Live cells stained with calcein AM yield a green fluorescence signal, whereas dead cells exhibit no fluorescence or a red signal due to the ethidium homodimer-1. As observed in Fig. 2, A2780 ovarian cancer cells treated with complex **1** (10  $\mu\text{M}$ ) for 48 h were mostly dead, whereas control cells without any drug treatment under the same conditions were alive. The  $\text{IC}_{50}$  for complex **1** against A2780 at 48 h is  $4.94 \pm 1.52 \mu\text{M}$ .

The cytotoxicity of the newly synthesized monofunctional complex **1** was next evaluated against a panel of four human cancer cell lines of different origin (A2780, ovarian cancer; A2780CP70, cisplatin-resistant ovarian cancer; MCF-7, breast cancer; HCT116, colorectal cancer) using the MTT [3-(4,5-dimethylthiazol-2-yl)-2,5-diphenyltetrazolium bromide] assay (Table 1). Cell viability was recorded after 72 h and compared to results obtained with cisplatin, oxaliplatin, and phenanthriplatin under identical conditions. Complex **1** displayed cytotoxicity similar to that of oxaliplatin but failed to perform as well as phenanthriplatin.

The selectivity of complex **1** for tumour cells over healthy cells was probed next. Normal lung fibroblasts (MRC5) and cancerous lung (A549) cells were used to evaluate the selectivity of complex **1** for cancer vs. healthy cells. Based on the MTT assay, the ratio of  $\text{IC}_{50}$  values in healthy MRC5 cells to those in cancerous A549 cells was 0.9 for cisplatin compared with 2.9 for complex **1**. The higher ratio obtained for complex **1** reveals its selectivity for cancer cells, at least in the cellular monolayer assays used in this study.

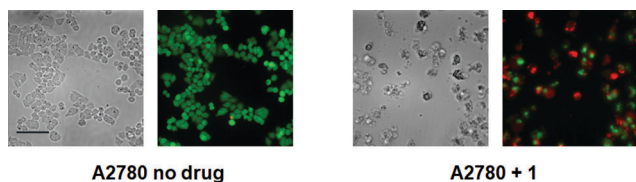


Fig. 2 Calcein AM/ethidium homodimer-1 cell viability assay, details of which may be found in the main text and ESI† (scale bar, 44  $\mu\text{m}$ ).

Table 1  $\text{IC}_{50}$  values<sup>a</sup> for cisplatin, oxaliplatin, phenanthriplatin and complex **1** in the various cell lines for a 72 h incubation period

$\text{IC}_{50}$ ( $\mu\text{M}$ )	A2780	A2780CP70	MCF-7	HCT116
Cisplatin	$1.7 \pm 1.0$	$9.9 \pm 2.1$	$9.0 \pm 3.2$	$16.8 \pm 5.1$
Oxaliplatin	$0.21 \pm 0.09$	$5.1 \pm 2.2$	$12.2 \pm 2.4$	$7.4 \pm 1.7$
Phenanthriplatin	$0.19 \pm 0.03$	$0.29 \pm 0.06$	$0.80 \pm 0.05$	$1.2 \pm 0.5$
<b>1</b>	$1.9 \pm 0.2$	$6.5 \pm 1.4$	$14.9 \pm 0.8$	$8.9 \pm 2.3$

<sup>a</sup> Data reflect the mean and standard deviation of results from three separate experiments, each performed in triplicate.

Next, we sought to quantitate the cellular uptake and the subcellular distribution of complex **1**. The nuclei, cytoplasm, membrane, and whole cell concentrations of platinum were measured by graphite furnace atomic absorption spectroscopy (GFAAS) after treatment of the cells with the compounds for 5 h (Fig. 3). Phenanthriplatin was used as a comparison, and oxaliplatin and cisplatin were used as controls. After 5 h incubation with the Pt compounds, phenanthriplatin and complex **1** were taken up by cells more effectively than cisplatin or oxaliplatin. These results reflect the ability of the larger, hydrophobic heterocyclic phenanthridine ligand to facilitate uptake of the phenanthriplatin and complex **1** cations through the cytoplasmic membrane. However, the uptake of phenanthriplatin is, surprisingly, much higher than that of complex **1**, indicating that geometric isomerism may play an important role in cellular uptake. Most of the platinum is found in the cytoplasm. The higher cellular uptake of phenanthriplatin most likely contributes to its enhanced cytotoxicity compared with the other platinum compounds.

DNA is the cellular target of platinum-based anticancer agents, thus the ability of complex **1** to platinate nuclear DNA was assessed. Two million HCT116 cells were treated with growth medium containing 20  $\mu\text{M}$  cisplatin, oxaliplatin, phenanthriplatin, or complex **1** for 5 h, followed by incubation in fresh media for an additional 16 h. The intracellular DNA was isolated and the quantity of bound platinum was measured by GFAAS. The extent of DNA platination was determined to be  $23.2 \pm 3.6$  Pt adducts per  $10^6$  nucleotides for cisplatin,  $6.7 \pm 1.0$  Pt adducts per  $10^6$  nucleotides for oxaliplatin,  $87.8 \pm 6.6$  Pt adducts per  $10^6$

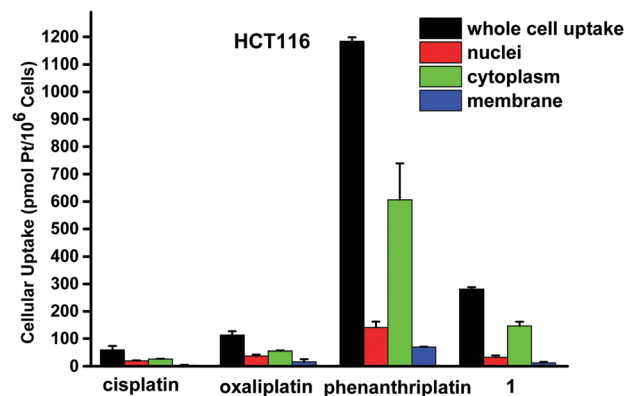


Fig. 3 Cellular distribution of Pt in HCT116 treated with cisplatin, oxaliplatin, phenanthriplatin and **1**. Cells were treated with 20  $\mu\text{M}$  platinum complex for 5 h. Platinum uptake is presented in units of pmol of Pt per  $10^6$  cells.



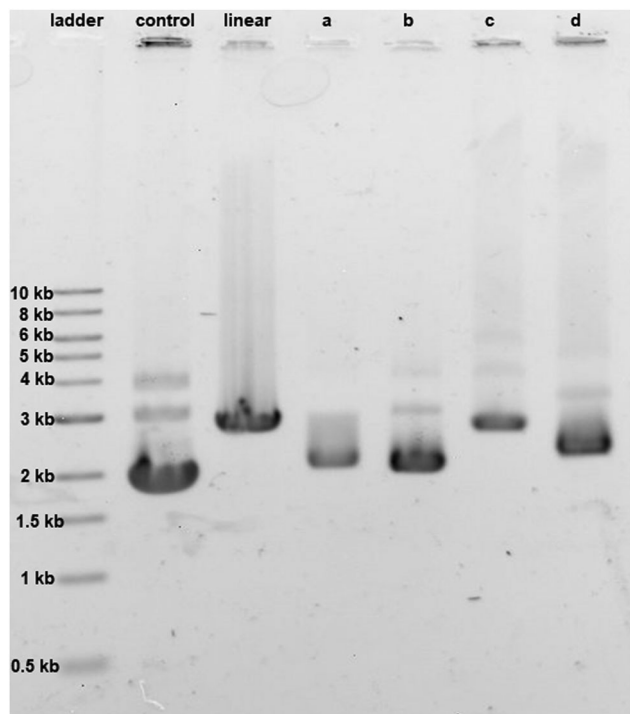


Fig. 4 Unwinding effect of  $30 \mu\text{g mL}^{-1}$  concentration of (a) cisplatin, (b) oxaliplatin, (c) phenanthriplatin, and (d) complex **1** on pUC19 DNA ( $15 \mu\text{g mL}^{-1}$ ). For control, no platinum compound was added; for linear, the pUC19 plasmid was restriction digested by HindIII.

nucleotides for phenanthriplatin, and  $6.3 \pm 1.6$  Pt adducts per  $10^6$  nucleotides for complex **1**.

The effect of cisplatin, oxaliplatin, phenanthriplatin, and complex **1** on supercoiled pUC19 DNA in Tris-HCl buffer (0.1 M, pH 7.4) at  $37^\circ\text{C}$  after incubating in the dark for 6 h was studied by agarose gel electrophoresis (Fig. 4). Comparing the migration of pUC19 in the presence of the different platinum agents we see that DNA modified by complex **1** behaves similarly to that modified by cisplatin and oxaliplatin. In contrast, migration of phenanthriplatin<sup>11</sup> treated DNA is consistent with relaxation of the negatively supercoiled plasmid in response to intercalation of, and/or photocleavage by, the phenanthridine ring.<sup>12,13</sup> Our results therefore indicate that both the choice of coordinating ligands as well as the stereochemistry at the platinum center dictate the ability of platinum compounds to unwind duplex DNA.<sup>14</sup>

$\gamma\text{H2AX}$ , the phosphorylated form of histone protein H2AX, is a known biomarker of DNA damage induced by platinum drugs.<sup>15,16</sup>  $\gamma\text{H2AX}$  can be detected by immunostaining. As shown in Fig. 5, fluorescence microscopy was used to visualize the localization of  $\gamma\text{H2AX}$  in the nucleus of HCT116 cells treated with complex **1**, indicating genomic DNA damage. Apoptotic cells normally exhibit changes in cell morphology, such as blebbing, chromatin condensation, and nuclear fragmentation, which can be observed by fluorescence microscopy. As shown in Fig. 5, morphological changes occur following treatment of HCT116 cells with  $20 \mu\text{M}$  complex **1** for 24 h. Chromatin condensation and nuclear fragmentation were also

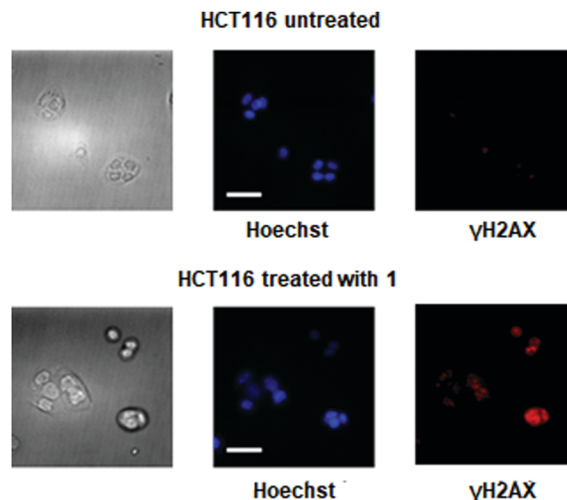


Fig. 5 DNA damage and cellular responses of HCT116 cells treated with complex **1**: cellular images, left; nuclear staining, blue; immunostaining of the biomarker of DNA damage, phosphorylatedH2AX ( $\gamma\text{H2AX}$ ), red (scale bar,  $30 \mu\text{m}$ ).

identified by Hoechst staining. All these cell-based experiments clearly indicate that complex **1** can effectively induce DNA damage and thus lead to cell cycle arrest and apoptosis in cancer cells.

Finally, intestinal organoids are three-dimensional primary cultures derived from intestinal stem cells that closely recapitulate the *in vivo* tissue structure.<sup>17</sup> As previously described, organoid cellular composition closely mimics *in vivo* biology in terms of secretory function, absorptive function, and pathophysiologic states.<sup>18</sup> Organoid assays have therefore gained in popularity for assessing drug toxicity and selectivity *in vivo*. Furthermore, organoid cultures are amenable for high-throughput drug

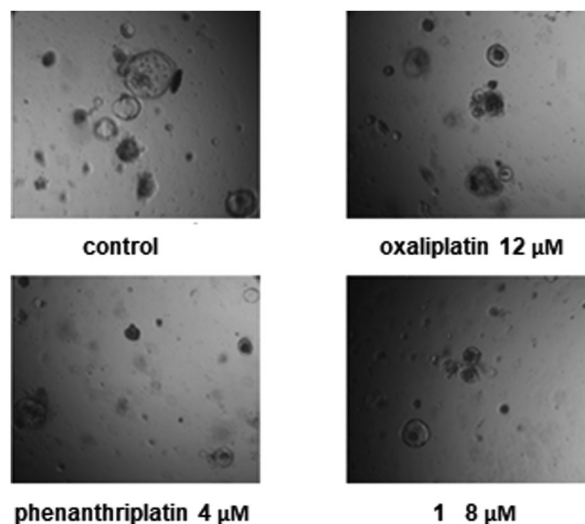


Fig. 6 Oxaliplatin, phenanthriplatin, and complex **1** inhibit AKP intestinal cancer organoid growth *in vitro* at different concentrations: (1) control AKP organoids exhibit a large cystic morphology, consistent with their highly proliferative and poorly differentiated state; (2) oxaliplatin, phenanthriplatin, and complex **1** induce organoid death, as shown by cell necrosis within the organoid lumen.



screening assays that can accurately predict *in vivo* outcomes.<sup>19</sup> The adenomatous polyposis coli (APC) gene product is essential for intestinal stem cell homeostasis as it regulates intracellular beta-catenin concentration and subsequent stem cell proliferation. Loss of function mutations in the APC gene occur as early events in a majority of colorectal cancers.<sup>20</sup> Additional oncogenic mutations such as those involving KRAS and TP53 subsequently occur and are associated with more aggressive tumor phenotypes, permitting local invasion and metastasis to lymph nodes and the liver.

To validate the efficacy of phenanthriplatin and complex **1**, we utilized the Apc-knockout Kras<sup>G12D</sup> p53-knockout (AKP) engineered mouse intestinal cancer organoid model. By quantifying organoid formation, morphology, and cell viability, we determined the cytotoxicity of each drug (Fig. 6). Phenanthriplatin and complex **1** both exhibited significantly lower IC<sub>50</sub> values than that of both oxaliplatin and cisplatin. Taken together, these findings indicate that complex **1** has enhanced potency in treating intestinal cancers compared to oxaliplatin. *In vivo* studies are needed in order to understand how these results reflect the potential use of complex **1** clinically.

In conclusion, by replacing one of the chloride ligands of *trans*-DDP with the phenanthridine ligand, the monofunctional Pt(II) complex **1** was successfully synthesized, and it functioned as an effective anticancer agent. The results of cellular uptake, DNA platination, and DNA unwinding studies show very different activities between phenanthriplatin and its geometric isomer complex **1**. This result indicates that the stereochemistry at the Pt(II) center may play a great role in affecting the properties of monofunctional platinum based anticancer agents.

This work was supported by grant CA034992 to S. J. L. and NIH grants AG045144, CA034992, CA211184 to O. H. Y. In addition, O. H. Y. is also a Pew-Stewart Scholar for Cancer Research and a Sidney Kimmel Scholar.

## Conflicts of interest

There are no conflicts to declare.

## Notes and references

- 1 T. W. Hambley, *Coord. Chem. Rev.*, 1997, **166**, 181.
- 2 G. Chu, *J. Biol. Chem.*, 1994, **269**, 787.
- 3 E. R. Jamieson and S. J. Lippard, *Chem. Rev.*, 1999, **99**, 2467.
- 4 D. W. Shen, L. M. Pouliot, M. D. Hall and M. M. Gottesman, *Pharmacol. Rev.*, 2012, **64**, 706.
- 5 T. C. Johnstone, G. Y. Park and S. J. Lippard, *Anticancer Res.*, 2014, **34**, 471.
- 6 G. Y. Park, J. J. Wilson, Y. Song and S. J. Lippard, *Proc. Natl. Acad. Sci. U. S. A.*, 2012, **109**, 11987.
- 7 D. Wang, G. Y. Zhu, X. H. Huang and S. J. Lippard, *Proc. Natl. Acad. Sci. U. S. A.*, 2010, **107**, 9584.
- 8 M. T. Gregory, G. Y. Park, T. C. Johnstone, Y.-S. Lee, W. Yang and S. J. Lippard, *Proc. Natl. Acad. Sci. U. S. A.*, 2010, **107**, 9584.
- 9 M. W. Kellinger, G. Y. Park, J. Chong, S. J. Lippard and D. Wang, *J. Am. Chem. Soc.*, 2013, **135**, 13054.
- 10 I. A. Riddell, K. Agama, G. Y. Park, Y. Pommier and S. J. Lippard, *ACS Chem. Biol.*, 2016, **11**, 2996.
- 11 K. S. Lovejoy, R. C. Todd, S. Zhang, M. S. McCormick, J. A. D'Aquino, J. T. Reardon, A. Sancar, K. M. Giacomini and S. J. Lippard, *Proc. Natl. Acad. Sci. U. S. A.*, 2008, **105**, 8902.
- 12 L. Gude, M. A.-J. Fernández, K. B. Grant and A. Lorente, *Bioorg. Med. Chem. Lett.*, 2002, **12**, 3135.
- 13 J. R. Choudhury and U. Bierbach, *Nucleic Acids Res.*, 2005, **33**, 5622.
- 14 M. V. Keck and S. J. Lippard, *J. Am. Chem. Soc.*, 1992, **114**, 3386.
- 15 P. L. Olive and J. P. Banath, *Cytometry, Part B*, 2009, **76B**, 79.
- 16 Y. R. Zheng, K. Suntharalingam, T. C. Johnstone, H. Yoo, W. Lin, J. G. Brooks and S. J. Lippard, *J. Am. Chem. Soc.*, 2014, **136**, 8790.
- 17 J. Roper, T. Tammela, N. M. Cetinbas, A. Akkad, A. Roghanian, S. Rickelt, M. Almeqdadi, K. Wu, M. A. Oberli, F. Sánchez-Rivera, Y. K. Park, X. Liang, G. Eng, M. S. Taylor, R. Azimi, D. Kedrin, R. Neupane, S. Beyaz, E. T. Sicinska, Y. Suarez, J. Yoo, L. L. Chen, L. Zukerberg, P. Katajisto, V. Deshpande, A. J. Bass, P. N. Tschlis, J. Lees, R. Langer, R. O. Hynes, J. Z. Chen, A. Bhutkar, T. Jacks and Ö. H. Yilmaz, *Nat. Biotechnol.*, 2017, **35**, 569.
- 18 A. Fatehullah, S. H. Tan and N. Barker, *Nat. Cell Biol.*, 2016, **18**, 246.
- 19 H. Gao, J. M. Korn, S. Ferretti, J. E. Monahan, Y. Wang, M. Singh, C. Zhang, C. Schnell, G. Yang, Y. Zhang, O. A. Balbin, S. Barbe, H. Cai, F. Casey, S. Chatterjee, D. Y. Chiang, S. Chuai, S. M. Cogan, S. D. Collins, E. Dammassa, N. Ebel, M. Embry, J. Green, A. Kauffmann, C. Kowal, R. J. Leary, J. Lehar, Y. Liang, A. Loo, E. Lorenzana, E. Robert McDonald Iii, M. E. McLaughlin, J. Merkin, R. Meyer, T. L. Naylor, M. Patawaran, A. Reddy, C. Roelli, D. A. Ruddy, F. Salangsang, F. Santacroce, A. P. Singh, Y. Tang, W. Tinetto, S. Tobler, R. Velazquez, K. Venkatesan, F. Von Arx, H. Q. Wang, Z. Wang, M. Wiesmann, D. Wyss, F. Xu, H. Bitter, P. Atadja, E. Lees, F. Hofmann, E. Li, N. Keen, R. Cozens, M. R. Jensen, N. K. Pryer, J. A. Williams and W. R. Sellers, *Nat. Med.*, 2015, **21**, 1318.
- 20 L. N. Kwong and W. F. Dove, *Adv. Exp. Med. Biol.*, 2009, **656**, 85.

